

# Bioelectrochemistry of Cytochrome *c* in a Closed Bipolar Electrochemical Cell

Alonso Gamero-Quijano,<sup>a</sup> Grégoire Herzog,<sup>b\*</sup> Micheál D Scanlon<sup>a,c\*</sup>

<sup>a</sup> The Bernal Institute and Department of Chemical Sciences, School of Natural Sciences, University of Limerick (UL), Limerick V94 T9PX, Ireland.

<sup>b</sup> Laboratoire de Chimie Physique et Microbiologie pour les Matériaux et l'Environnement (LCPME), UMR 7564, CNRS, Université de Lorraine, 405 rue de Vandoeuvre, Villers-lès-Nancy, F-54600, France.

<sup>c</sup> Advanced Materials and Bioengineering Research (AMBER) Centre, Ireland.

\*Corresponding authors:

[gregoire.herzog@univ-lorraine.fr](mailto:gregoire.herzog@univ-lorraine.fr)

[micheal.scanlon@ul.ie](mailto:micheal.scanlon@ul.ie)

## Abstract

The reversible oxidation and reduction of Cytochrome *c* (Cyt *c*) is demonstrated with a closed bipolar electrochemical cell (CBPEC). Herein, a 4-electrode configuration was studied with the opposite poles of the bipolar electrode resting in separate aqueous and organic electrolyte solutions, respectively. Using biocompatible indium tin oxide (ITO) slides as the bipolar electrode poles, we investigated the influence of the redox potential of the reductant (decamethylferrocene or dimethylferrocene) in an  $\alpha,\alpha,\alpha$ -trifluorotoluene organic phase on the observed voltammetry. Reversible electron transfer was only observed between Cyt *c* and decamethylferrocene. Use of the weaker dimethylferrocene as the reductant required a larger external bias of the driving electrodes to initiate the electron transfer reaction between the two poles of the bipolar electrode. Consequently, the surface of the ITO slide at the aqueous pole experienced a significant negative cathodic potential and underwent irreversible reduction. The biphasic setup using the 4-electrode CBPEC provides insights into electron transfer processes at an interface between two immiscible electrolyte solutions (ITIES), highlighting the strong probability of observing

interfacial electron transfer between decamethylferrocene (but not dimethylferrocene) and Cyt *c* within the short  $\sim 1$  V polarisable potential window available at an ITIES.

## Keywords

Bipolar electrochemistry, four electrode configuration, bipolar electrode, Cytochrome *c*, bioelectrochemistry

## 1. Introduction

Direct electron transfer (DET) to redox proteins from conducting materials is of fundamental interest in mechanistic studies in biochemistry [1,2]. Optimisation of such charge transfer processes is central to the development of nanobiotechnological devices, such as biosensors for health monitoring or enzymatic fuel cells [3–5]. Cytochrome *c* (Cyt *c*) is a particularly well studied, relatively small (104 amino acid residues), redox protein due to its essential role in both mitochondrial electron transport and intrinsic type II apoptosis [6]. Cyt *c* is capable of DET between its heme co-factor and suitably modified electron conducting materials [7]. Bipolar electrochemistry involves the generation of simultaneous asymmetric electrochemical reactions at the opposite ends of isolated conductive objects, known as bipolar electrodes (BPEs), immersed in electrolyte solutions in the presence of an applied electric field [8–12]. In this study, the bioelectrochemistry of Cyt *c* was investigated using immiscible aqueous-organic electrolyte solutions in a 4-electrode closed bipolar electrochemical cell (CBPEC) configuration [13–22].

The BPE studied consisted of two indium tin oxide (ITO) slides, known to be electrochemically biocompatible with Cyt *c* [23,24], connected by an electric wire. The lipophilic species were dimethylferrocene (DiMFC), a weak reductant, and decamethylferrocene (DcMFC), a strong reductant. To successfully achieve bioelectrochemistry in a 4-electrode CBPEC configuration, we demonstrate that considerations such as the stability of the BPE across the polarisable potential window must be taken into account. We show that when the weaker DiMFC reductant is used, the large external biasing of the driving electrodes, *i.e.*, changing the applied Galvani potential difference ( $\Delta_o^W \phi$ ), required to initiate the electron transfer reaction establishes an equilibrium Galvani potential difference ( $\Delta_o^W \phi_{eq}$ ) of sufficient magnitude to reduce the ITO surface at the aqueous pole.

The interaction of Cyt *c* with lipophilic redox species is interesting as Cyt *c* undergoes redox chemistry with species present in a lipophilic membrane environment in the electron transport chain of mitochondria. The latter involves Cyt *c* shuttling electrons between Complexes III (Coenzyme Q – Cyt *c* reductase) and IV (Cyt *c* oxidase). Thus, in line with previous uses of this technique [13–22], our primary motivation is to acquire mechanistic insights for future studies of electron transfer events involving Cyt *c* at the interface between two immiscible electrolyte solutions (ITIES), considered a simple model system that mimics biological interfacial processes. Thus, the work herein highlights the under-utilised technique of 4-electrode closed bipolar electrochemistry with immiscible aqueous-organic solutions to study redox reactions between lipophilic redox species and aqueous redox active proteins. The latter reactions are inaccessible using typical 3-electrode bioelectrochemical experiments carried out in homogeneous aqueous conditions.

## 2. Experimental methods

### 2.1 3-electrode electrochemical cell experiments

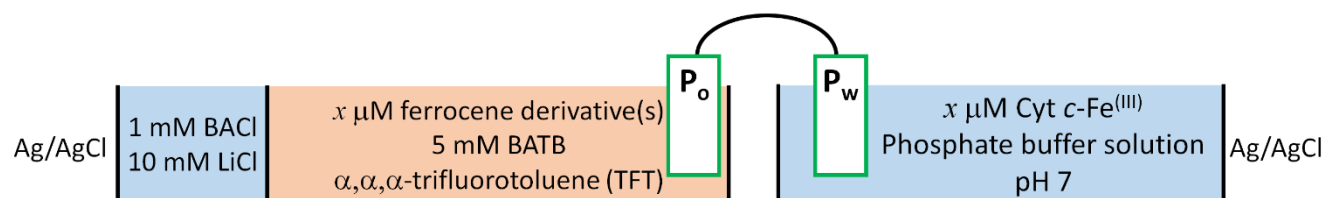
The materials used in this work are detailed in section S1.1, Supplementary Information (SI). All electrochemical measurements were obtained using an Autolab PGSTAT204 potentiostat from Metrohm, Switzerland. All 3-electrode electrochemistry experiments were performed in a home-made electrochemical cell designed for low volumes (< 5 mL). The working electrode was an ITO slide (area of 1 cm<sup>2</sup> and resistivity of 120 Ω); the electron conductor used to create the BPE. The ITO slides were rinsed and sonicated in acetone prior to electrochemical measurements. The counter electrode was a Pt wire and the reference electrode was a silver/silver chloride (Ag/AgCl) wire. Cyclic voltammograms (CVs) obtained in aqueous phosphate buffer solutions with a 3-electrode cell using Ag/AgCl reference electrodes were calibrated to the SHE scale as described in Fig. S1, section S1.2, SI.

Electrochemistry in the organic solvent  $\alpha,\alpha,\alpha$ -trifluorotoluene (TFT) required a slight modification of the electrochemical cell, with the Ag/AgCl electrode immersed in an “organic reference solution” that established a liquid junction with the organic phase. The organic reference solution was an aqueous solution of 1 mM LiCl and 10 mM BACl. CVs obtained in TFT solutions with a 3-electrode cell using Ag/AgCl reference electrodes were also calibrated to the SHE scale using the ferrocene (Fc<sup>+</sup>/Fc)

redox couple in TFT. The redox potential of the latter in TFT *versus* SHE has been determined previously as 0.720 V [25]. All experiments were carried out under aerobic conditions.

## 2.2 4-electrode CBPEC experiments with aqueous-organic electrolyte solutions

A schematic of the 4-electrode CBPEC with aqueous-organic electrolyte solutions experimental setup is shown in Scheme 1. The BPE consisted of two ITO slides, one in each compartment acting as the aqueous pole ( $P_w$ ) or organic pole ( $P_o$ ), respectively, and connected with an electric wire. Each compartment contained a Pt wire driving electrode and a Ag/AgCl reference electrode. In the organic compartment, the Ag/AgCl wire was immersed in an organic reference solution. The 4 electrodes were connected in an identical manner to that described for electrochemical measurements at the ITIES, see section S1.3, SI. It is important to note that for electron transfer experiments at the ITIES and 4-electrode CBPEC are thermodynamically equivalent. All experiments were carried out under aerobic conditions.



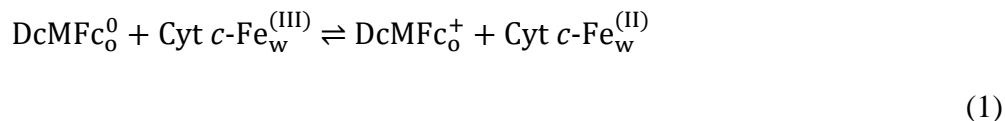
**Scheme 1.** Schematic of the 4-electrode CBPEC with aqueous-organic electrolyte solutions. The BPE consisted of two ITO slides connected by an electric wire, one in each compartment acting as the aqueous pole ( $P_w$ ) or organic pole ( $P_o$ ), respectively. The ferrocene derivatives studied in the TFT organic phase were DiMFc and DcMFc.

As is the case for electrochemical measurements at the ITIES, the applied potential ( $E$ ) in the 4-electrode CBPEC configuration with aqueous-organic electrolyte solutions is related to the Galvani potential scale by the relationship:  $E = \Delta_o^w \phi + \Delta E_{\text{ref}}$ . As the reference electrodes used at the ITIES and the 4-electrode CBPEC configuration are identical, the value of  $\Delta E_{\text{ref}}$  determined using a model ion transfer probe (tetramethylammonium cations,  $\text{TMA}^+$ ) at the ITIES can also be used to calibrate all voltammetry data obtained in the 4-electrode CBPEC configuration to the Galvani potential scale, see section S1.3, SI.

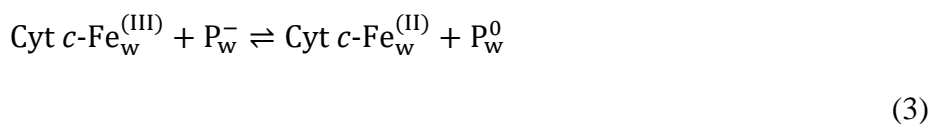
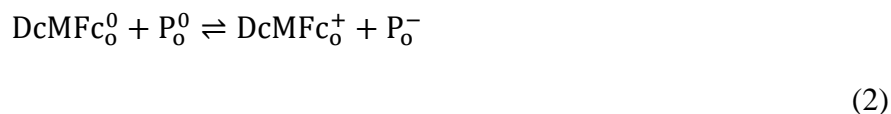
## 3. Results and Discussion

### 3.1 Voltammetry of Cyt *c* in a 4-electrode closed bipolar electrochemical cell

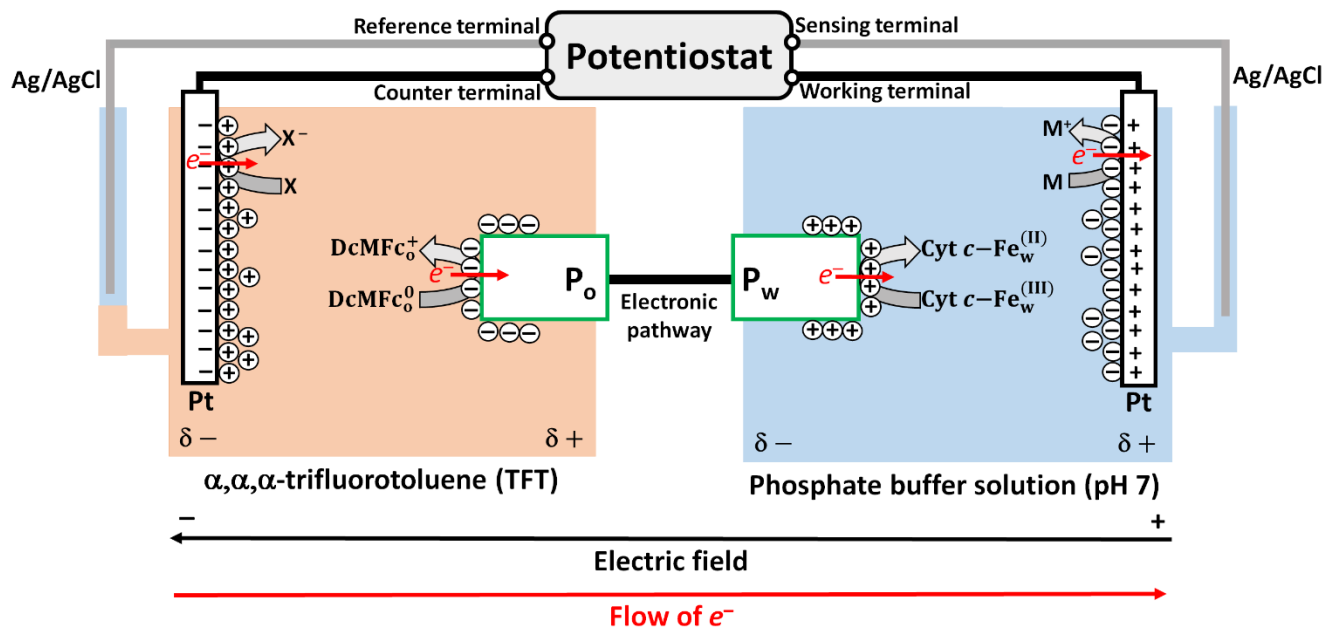
The configuration of the 4-electrode CBPEC used for the study of Cyt *c* bioelectrochemistry with aqueous-organic electrolyte solutions is illustrated in Scheme 1. Overall, the heterogeneous redox reaction is:



In the organic compartment,  $\text{DcMFC}_0$  will be oxidised at  $\text{P}_o$ , see Equation (2), with the concurrent reduction of molecule X (*e.g.*, a solvent molecule) at the surface of the organic driving electrode maintaining electroneutrality. Simultaneously, in the aqueous compartment,  $\text{Cyt } c\text{-Fe}_w^{(\text{III})}$  will be reduced at  $\text{P}_w$ , see Equation (3), with oxidation of molecule M at the surface of the aqueous driving electrode (see Scheme 2).



The current convention for electrochemical experiments with a 4-electrode CBPEC is explained in section 1.4, SI.



**Scheme 2.** Schematic of the 4-electrode CBPEC configuration with aqueous-organic electrolyte solutions used for the study of Cyt *c* bioelectrochemistry as  $\Delta_o^w \phi$  is biased sufficiently positively by the potentiostat to facilitate electron transfer along the BPE from the organic electron donor DcMFC at P<sub>o</sub> to the aqueous Cyt *c* molecule at P<sub>w</sub>.

The redox potential of the Cyt *c*-Fe<sup>(III)</sup>/Cyt *c*-Fe<sup>(II)</sup> couple in phosphate buffer solution at pH 7 *versus* SHE ( $\left[ E_{\text{Cyt } c\text{-Fe}_w^{(III)}/\text{Cyt } c\text{-Fe}_w^{(II)}}^{\ominus} \right]_{\text{SHE}}^w$ ) was determined as +0.267 V (Fig. S2(A), section 2, SI) and the redox potentials of the DcMFC<sup>+</sup>/DcMFC ( $\left[ E_{\text{DcMFC}_o^+/\text{DcMFC}_o^0}^{\ominus} \right]_{\text{SHE}}^o$ ) and DiMFC<sup>+</sup>/DiMFC ( $\left[ E_{\text{DiMFC}_o^+/\text{DiMFC}_o^0}^{\ominus} \right]_{\text{SHE}}^o$ ) couples in TFT *versus* SHE were determined as +0.107 V and +0.584 V, respectively (Fig. S2(B), section 2, SI). Thermodynamically, the standard Galvani potential difference for the heterogeneous electron transfer (HET), given by  $\Delta_o^w \phi_{\text{HET}}^{\ominus} = \left( \left[ E_{\text{DcMFC}_o^+/\text{DcMFC}_o^0}^{\ominus} \right]_{\text{SHE}}^o - \left[ E_{\text{Cyt } c\text{-Fe}_w^{(III)}/\text{Cyt } c\text{-Fe}_w^{(II)}}^{\ominus} \right]_{\text{SHE}}^w \right)$ , represents the potential where the redox reaction described in Equation (1) is at equilibrium and, therefore, any differential variation in potential would shift the equilibrium to the left or right. This equilibrium potential is assumed to be the half-wave potential of the reversible redox process ( $\Delta_o^w \phi_{1/2}$ ) recorded with the 4-electrode CBPEC [22]. Thus, with DcMFC as the lipophilic reductant  $\Delta_o^w \phi_{\text{HET}}^{\ominus} = -0.160$  V and with DiMFC  $\Delta_o^w \phi_{\text{HET}}^{\ominus} = +0.317$  V.

The  $\Delta_o^w \phi_{1/2}$  values recorded with the 4-electrode CBPEC for Cyt *c* reduction by the DcMFC and DiMFC redox couples, respectively, were expected to be separated by approximately 0.477 V, corresponding to the differences in their measured redox potentials using the 3-electrode cells. Thus, the CVs were predicted to exhibit a pair of well-resolved redox responses, with the response at the more positive  $\Delta_o^w \phi$  value attributable to the weaker DiMFC reductant. A CV using the 4-electrode CBPEC configuration detailed in Scheme 1 was obtained with 8  $\mu\text{M}$  Cyt *c* in the phosphate buffer solution and both 14  $\mu\text{M}$  DiMFC and 14  $\mu\text{M}$  DcMFC in the TFT organic electrolyte (Fig. 1(A), solid red line). Indeed, a pair of well-resolved redox responses were observed. However, only one showed a reversible character at  $-0.161$  V, with the redox response at the more positive potential of  $+0.271$  V being irreversible. Furthermore, the theoretically expected separation between the redox signals of  $+0.477$  V was not observed, with a smaller separation of  $0.432$  V measured (Fig. 1(A), solid red line).

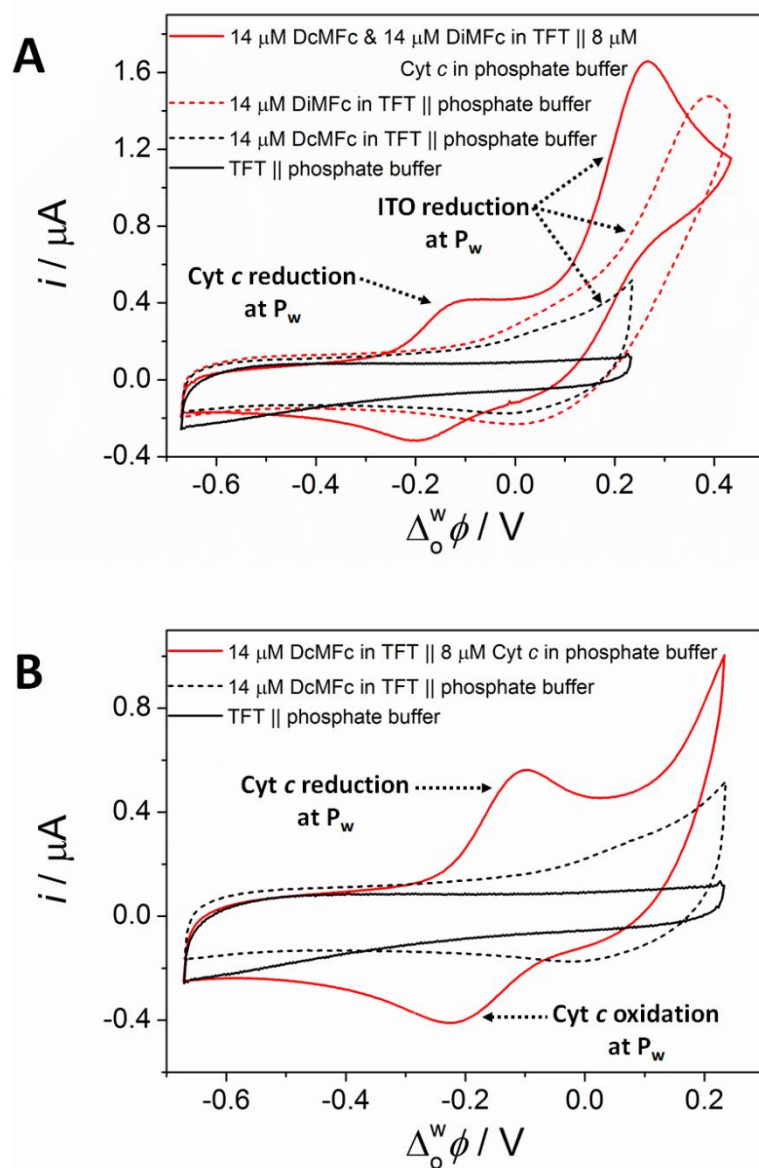


**Fig. 1. (A)** CVs obtained using the 4-electrode CBPEC configuration with aqueous-organic electrolyte solutions outlined in Scheme 1, in the absence of Cyt *c* and both ferrocene derivatives (solid black line), in the presence of 14  $\mu\text{M}$  DcMFC only (dashed black line), in the presence of 14  $\mu\text{M}$  DiMFc only (dashed red line), and in the presence of 8  $\mu\text{M}$  Cyt *c*, 14  $\mu\text{M}$  DiMFc and 14  $\mu\text{M}$  DcMFC (solid red line). The scan rate used was  $20 \text{ mV}\cdot\text{s}^{-1}$ . **(B)** CVs obtained using the 4-electrode CBPEC configuration outlined in Scheme 1, as described in (A), using a smaller polarisable potential window to clearly observe the redox response at  $\Delta_0^w \phi_{1/2} = -0.161 \text{ V}$  in the presence of 8  $\mu\text{M}$  Cyt *c* and 14  $\mu\text{M}$  DcMFC (solid red line). The scan rate used was  $20 \text{ mV}\cdot\text{s}^{-1}$ .

The irreversible positive peak recorded at +0.271 V (Fig. 1(A)) was attributed to the reduction of the ITO electrode acting as  $P_w$ . ITO is known to undergo morphological changes and dissolve on application of moderately negative cathodic potentials when used as the working electrode in a 3-electrode cell [26–28]. The sensitivity of the ITO electrodes to electrochemical reduction under the experimental conditions present in the aqueous compartment of the 4-electrode CBPEC (phosphate buffer solution at pH 7, as described in Scheme 1) is demonstrated in Fig. S3, section 3, SI. Control experiments in the absence of Cyt  $c$  revealed that ITO reduction began when  $\Delta_o^w \phi$  exceeded 0 V with both DiMFC (Fig. 1(A), red dashed line) and DcMFC (Fig. 1(A), black dashed line) in the TFT organic electrolyte. Interestingly, as both DcMFC and DiMFC were active in reducing the ITO electrode, the irreversible ITO reduction peak was observed at a lower potential when both were present in the organic compartment (Fig. 1(A), solid red line), than solely with DiMFC present (Fig. 1(A), dashed red line). Thus, the reversible redox response observed in the presence of Cyt  $c$  at  $\Delta_o^w \phi_{1/2} = -0.161$  V is the sole electrochemical signal in Fig. 1(A) attributed to the redox chemistry of Cyt  $c$  in the 4-electrode CPBEC experiment. The experimental result with DiMFC in the organic phase and Cyt  $c$  in the aqueous phase was not shown as it is identical to that of DiMFC in the organic phase and no Cyt  $c$  in the aqueous phase (Fig. 1a, red dashed line).

For clarity, this signal is presented in a smaller polarisable potential window that avoids ITO reduction, with the necessary control experiments also shown, in Fig. 1(B). No redox response is observed at  $-0.161$  V in the absence of Cyt  $c$  with either DcMFC (Fig. 1(A) and (B), dashed black lines) or DiMFC (Fig. 1(A), dashed red line) in the TFT organic electrolyte. Furthermore, the observed  $\Delta_o^w \phi_{1/2}$  value matches very well with the  $\Delta_o^w \phi_{\text{HET}}^\ominus$  value of  $-0.160$  V for Cyt  $c$  reduction by DcMFC predicted earlier from the redox potentials measured using the 3-electrode setup.

### 3.2 Comparing the voltammetry obtained using a conventional 3-electrode cell to that obtained with a 4-electrode closed bipolar electrochemical cell

By comparison with the redox response of Cyt  $c$  at an ITO working electrode using a conventional 3-electrode cell with a Ag/AgCl reference electrode, the reversible redox response observed at  $\Delta_o^w \phi_{1/2} = -0.161$  V on the Galvani scale using the 4-electrode CPBEC with DcMFC in the TFT organic electrolyte was unambiguously attributed to the redox chemistry of Cyt  $c$ . To achieve such a comparison, shown in Fig. 2(A), the aqueous Ag/AgCl reference electrode potential scale was linked to the DcMFC potential scale in the TFT organic electrolyte, against which all reduction processes are occurring in the 4-electrode



CBPEC [16], as rationalized in section S4, SI. With DcMFC, a net offset *versus* the interfacial Galvani potential difference ( $\Delta_o^w \phi_{\text{Offset}}$ ) of  $-0.219$  V was determined (section S4, SI). The precise overlap for the redox response at  $\Delta_o^w \phi_{1/2} = -0.161$  V confirms that electron transfer along the BPE between DcMFC and Cyt *c* is taking place as described in Equations (2) and (3).

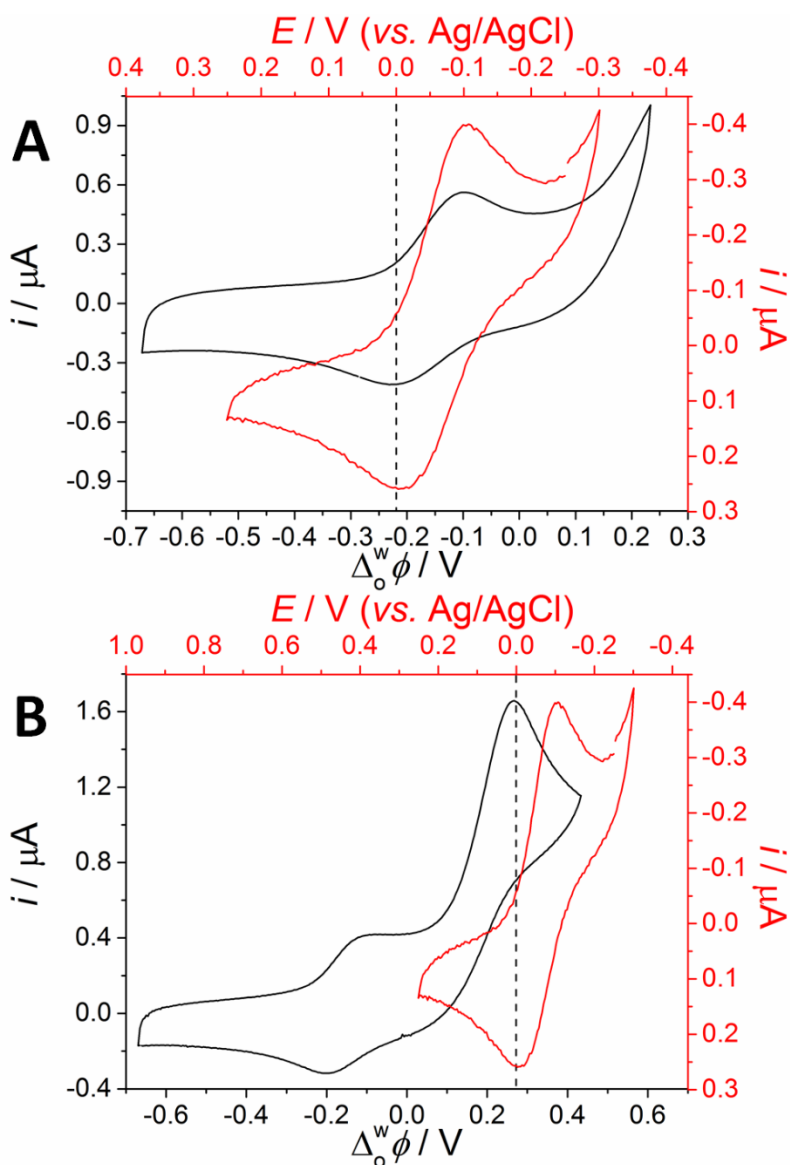


**Fig. 2.** Comparison of CVs recorded using the 4-electrode CBPEC with aqueous-organic electrolyte solutions outlined in Scheme 1 in the presence of (A) 8  $\mu\text{M}$  Cyt *c* and 14  $\mu\text{M}$  DcMFC (solid black line) or (B) 8  $\mu\text{M}$  Cyt *c*, 14  $\mu\text{M}$  DiMFC and 14  $\mu\text{M}$  DcMFC (solid black line) and a CV recorded using a 3-electrode cell with 8  $\mu\text{M}$  Cyt *c* in phosphate buffer solution at pH 7 (solid red line). The aqueous Ag/AgCl reference electrode potential scale was linked to the DcMFC potential scale in the TFT organic electrolyte, as

described in the text, in (A) and linked to the DiMFC potential scale in (B). All CVs were obtained at 20  $\text{mV}\cdot\text{s}^{-1}$ .

Using this approach, the aqueous Ag/AgCl reference electrode potential scale was also linked to the DiMFC potential scale in the TFT organic electrolyte, and in this case  $\Delta_o^w \phi_{\text{offset}}$  was +0.272 V. The comparison of the redox response of Cyt *c* measured using a 3-electrode cell with a Ag/AgCl reference electrode and the irreversible redox response observed in the presence of Cyt *c* at  $\Delta_o^w \phi_{1/2} = +0.271$  V on the Galvani potential scale using the 4-electrode CPBEC with DcMFC and DiMFC in the TFT organic electrolyte is presented in Fig. 2(B). The lack of an overlap for the redox response at  $\Delta_o^w \phi_{1/2} = +0.271$  V indicates that the redox response at this potential is not attributable to Cyt *c* reduction. This is in agreement with the earlier findings that the redox response at  $\Delta_o^w \phi_{1/2} = +0.271$  V is due to ITO reduction

Finally, if an electron transfer is recorded with a 4-electrode CBPEC between an aqueous acceptor and organic donor redox species, and the signal is within the Galvani potential window of  $-0.4$  to  $+0.6$  V (the upper and lower limits currently available at an ITIES formed between aqueous and TFT electrolytes), there is a high probability that electron transfer will be recorded at the ITIES. For DcMFC, the  $\Delta_o^w \phi_{1/2}$  value determined of  $-0.161$  V indicates that interfacial electron transfer at an ITIES between DcMFC and Cyt *c* may be observable within the potential window. However, for DiMFC, the calculated  $\Delta_o^w \phi_{\text{HET}}^{\ominus}$  of  $+0.317$  V, indicates that interfacial electron transfer between DiMFC and Cyt *c* is likely to occur beyond the potential window at more positive potentials. This is because significant additional overpotentials to interfacial electron transfer across the mixed solvent region at the ITIES, *e.g.*, reorganisation energies and double-layer effects [20,25], are expected in comparison to the much less inhibited kinetics of heterogeneous electron transfer along a conductive BPE in the 4-electrode CBPEC or a working electrode in a 3-electrode cell. These overpotentials will push the  $\Delta_o^w \phi_{1/2}$  values expected for the interfacial electron transfer more positive. Thus, our findings cast doubt on previous articles reporting interfacial electron transfer between Cyt *c* and DiMFC at the ITIES with  $\Delta_o^w \phi_{1/2}$  values of  $\sim 0.100$  V [29,30]. In this regard, experimental studies to re-visit the feasibility of observing interfacial electron transfer at the ITIES between Cyt *c* and either DcMFC or DiMFC in the organic electrolyte are now underway.

## 4. Conclusions

Herein, direct electron transfer between Cyt *c* and the aqueous pole of a bipolar electrode in a 4-electrode closed bipolar electrochemical cell (CBPEC) with aqueous-organic electrolyte solutions is demonstrated. The stability of the aqueous ITO pole was linked to the redox potential of the organic electron donor species (either decamethylferrocene or dimethylferrocene). The larger the difference between the redox potentials of the ferrocene-derivative and Cyt *c*, the greater the required external bias of the driving electrodes. Thus, the large external bias required when using the weaker reductant, dimethylferrocene, led to irreversible reduction of the ITO at the aqueous pole during the 4-electrode CBPEC experiment. The latter is demonstrated as a viable alternative experimental approach to the conventional 3-electrode cell to explore the bioelectrochemistry of Cyt *c*, especially using lipophilic reductants or oxidants. In this sense, ample opportunities exist to test the biocompatibility of surface modifications to the aqueous pole of the bipolar electrode, such as through the use of self-assembled monolayers on gold, lipid membranes, advanced carbon nanomaterials, or conductive polymers, to prevent protein denaturation on contact with the electrode surface. A major perspective is to confirm the predicted observation of interfacial electron transfer at the ITIES between decamethylferrocene and Cyt *c* within the available potential window. The use of the soft interface at an ITIES, mirroring soft biomembranes, to monitor bioelectrochemical reactions with redox active proteins would be of major interest.

## Acknowledgements

This publication has emanated from research by M. D. S. supported by the European Research Council through a Starting Grant (agreement no. 716792) and in part by a research grant from Science Foundation Ireland (SFI) (grant number 13/SIRG/2137). A. G.-Q. acknowledges funding received from an Irish Research Council Government of Ireland Postdoctoral Fellowship Award (grant number GOIPD/2018/252). G. H. is grateful to the French Programme Investissement d'Avenir (PIA) "Lorraine Université d'Excellence" (Reference No. ANR-15-IDEX-04-LUE). for the partial financial support of this work. The authors are grateful to the support of the Irish Research Council and Campus France for travel support between the French and Irish groups through their joint ULYSSES programme.

## References

- [1] C. Léger, P. Bertrand, Direct Electrochemistry of Redox Enzymes as a Tool for Mechanistic

- Studies, *Chem. Rev.* 108 (2008) 2379–2438. doi:10.1021/cr0680742.
- [2] F.A. Armstrong, H.A.O. Hill, N.J. Walton, Direct electrochemistry of redox proteins, *Acc. Chem. Res.* 21 (1988) 407–413. doi:10.1021/ar00155a004.
- [3] C.D. Bostick, S. Mukhopadhyay, I. Pecht, M. Sheves, D. Cahen, D. Lederman, Protein bioelectronics: a review of what we do and do not know, *Reports Prog. Phys.* 81 (2018) 026601. doi:10.1088/1361-6633/aa85f2.
- [4] A. Walcarius, S.D. Minter, J. Wang, Y. Lin, A. Merkoçi, Nanomaterials for bio-functionalized electrodes: Recent trends, *J. Mater. Chem. B.* 1 (2013) 4878–4908. doi:10.1039/c3tb20881h.
- [5] D. Leech, P. Kavanagh, W. Schuhmann, Enzymatic fuel cells: Recent progress, *Electrochim. Acta.* 84 (2012) 223–234. doi:10.1016/j.electacta.2012.02.087.
- [6] M. Hüttemann, P. Pecina, M. Rainbolt, T.H. Sanderson, E. Valerian, L. Samavati, J.W. Doan, I. Lee, The multiple functions of cytochrome c and their regulation in life and death decisions of the mammalian cell: from respiration to apoptosis, *Mitochondrion.* 11 (2011) 369–381. doi:10.1016/j.mito.2011.01.010.The.
- [7] S.S. Seyedi, M.M. Waskasi, D. V. Matyushov, Theory and Electrochemistry of Cytochrome c, *J. Phys. Chem. B.* 121 (2017) 4958–4967. doi:10.1021/acs.jpcc.7b00917.
- [8] J.C. Bradley, H.M. Chen, J. Crawford, J. Eckert, K. Ernazarova, T. Kurzeja, M. Lin, M. McGee, W. Nadler, S.G. Stephens, Creating electrical contacts between metal particles using directed electrochemical growth, *Nature.* 389 (1997) 268–271. doi:10.1038/38464.
- [9] S.E. Fosdick, K.N. Knust, K. Scida, R.M. Crooks, Bipolar electrochemistry, *Angew. Chemie - Int. Ed.* 52 (2013) 10438–10456. doi:10.1002/anie.201300947.
- [10] G. Loget, D. Zigah, L. Bouffier, N. Sojic, A. Kuhn, Bipolar electrochemistry: from materials science to motion and beyond, *Acc. Chem. Res.* 46 (2013) 2513–2523. doi:10.1021/ar400039k.
- [11] C.A.C. Sequeira, D.S.P. Cardoso, M.L.F. Gameiro, Bipolar Electrochemistry, a Focal Point of Future Research, *Chem. Eng. Commun.* 203 (2016) 1001–1008. doi:10.1080/00986445.2016.1147031.
- [12] L. Koefoed, S.U. Pedersen, K. Daasbjerg, Bipolar electrochemistry—A wireless approach for electrode reactions, *Curr. Opin. Electrochem.* 2 (2017) 13–17. doi:10.1016/j.coelec.2017.02.001.

- [13] D. Plana, F.G.E. Jones, R.A.W. Dryfe, The voltammetric response of bipolar cells: Reversible electron transfer, *J. Electroanal. Chem.* 646 (2010) 107–113. doi:10.1016/j.jelechem.2010.03.020.
- [14] H. Hotta, N. Akagi, T. Sugihara, S. Ichikawa, T. Osakai, Electron-conductor separating oil-water (ECSOW) system: A new strategy for characterizing electron-transfer processes at the oil/water interface, *Electrochem. Commun.* 4 (2002) 472–477. doi:10.1016/S1388-2481(02)00343-0.
- [15] H. Hotta, S. Ichikawa, T. Sugihara, T. Osakai, Clarification of the Mechanism of Interfacial Electron-Transfer Reaction between Ferrocene and Hexacyanoferrate(III) by Digital Simulation of Cyclic Voltammograms, *J. Phys. Chem. B.* 107 (2003) 9717–9725. doi:10.1021/jp035058p.
- [16] Y. Gründer, M.D. Fabian, S.G. Booth, D. Plana, D.J. Fermín, P.I. Hill, R.A.W. Dryfe, Solids at the liquid–liquid interface: Electrocatalysis with pre-formed nanoparticles, *Electrochim. Acta.* 110 (2013) 809–815. doi:10.1016/j.electacta.2013.03.185.
- [17] S. Wu, Z. Zhou, L. Xu, B. Su, Q. Fang, Integrating bipolar electrochemistry and electrochemiluminescence imaging with microdroplets for chemical analysis, *Biosens. Bioelectron.* 53 (2014) 148–153. doi:10.1016/j.bios.2013.09.042.
- [18] A. Uehara, T. Hashimoto, R.A.W. Dryfe, Au Electrodeposition at the Liquid-Liquid Interface: mechanistic aspects, *Electrochim. Acta.* 118 (2014) 26–32. doi:10.1016/j.electacta.2013.11.162.
- [19] N. Nishi, T. Kakinami, T. Sakka, Dendritic nanofibers of gold formed by the electron transfer at the interface between water and a highly hydrophobic ionic liquid, *Chem. Commun.* 51 (2015) 13638–13641. doi:10.1039/c5cc05476a.
- [20] E. Smirnov, P. Peljo, M.D. Scanlon, H.H. Girault, Gold Nanofilm Redox Catalysis for Oxygen Reduction at Soft Interfaces, *Electrochim. Acta.* 197 (2016) 362–373. doi:10.1016/j.electacta.2015.10.104.
- [21] J.D. Zhang, N. Hao, L. Lu, S. Yun, X.F. Zhu, K. Hong, L.D. Feng, High-efficient preparation and screening of electrocatalysts using a closed bipolar electrode array system, *J. Electroanal. Chem.* 832 (2019) 1–6. doi:10.1016/j.jelechem.2018.10.025.
- [22] A. Gamero-Quijano, A.F. Molina-Osorio, P. Peljo, M.D. Scanlon, Closed bipolar electrochemistry in a four-electrode configuration, *Phys. Chem. Chem. Phys.* 21 (2019) 9627–9640. doi:10.1039/C9CP00774A.

- [23] A. El Kasmi, M.C. Leopold, R. Galligan, R.T. Robertson, S.S. Saavedra, K. El Kacemi, E.F. Bowden, Adsorptive immobilization of cytochrome c on indium / tin oxide ( ITO ): electrochemical evidence for electron transfer-induced conformational changes, *Electrochem. Commun.* 4 (2002) 177–181. doi:10.1016/S1388-2481(01)00299-5.
- [24] N. Matsuda, J.H. Santos, A. Takatsu, K. Kato, Spectroelectrochemical studies on surface immobilized cytochrome c on ITO electrode by slab optical waveguide spectroscopy, *Thin Solid Films.* 438–439 (2003) 403–406. doi:10.1016/S0040-6090(03)00788-0.
- [25] E. Smirnov, P. Peljo, M.D. Scanlon, H.H. Girault, Interfacial Redox Catalysis on Gold Nanofilms at Soft Interfaces, *ACS Nano.* 9 (2015) 6565–6575. doi:10.1021/acs.nano.5b02547.
- [26] M. Senthilkumar, J. Mathiyarasu, J. Joseph, K.L.N. Phani, V. Yegnaraman, Electrochemical instability of indium tin oxide (ITO) glass in acidic pH range during cathodic polarization, *Mater. Chem. Phys.* 108 (2008) 403–407. doi:10.1016/j.matchemphys.2007.10.030.
- [27] L. Liu, S. Yellinek, I. Valdinger, A. Donval, D. Mandler, Important Implications of the Electrochemical Reduction of ITO, *Electrochim. Acta.* 176 (2015) 1374–1381. doi:10.1016/j.electacta.2015.07.129.
- [28] S. Geiger, O. Kasian, A.M. Mingers, K.J.J. Mayrhofer, S. Cherevko, Stability limits of tin-based electrocatalyst supports, *Sci. Rep.* 7 (2017) Article number: 4595. doi:10.1038/s41598-017-04079-9.
- [29] Y. Imai, T. Sugihara, T. Osakai, Electron Transfer Mechanism of Cytochrome cat the Oil/Water Interface as a Biomembrane Model, *J. Phys. Chem. B.* 116 (2012) 585–592. doi:10.1021/jp2092658.
- [30] G.C. Lillie, S.M. Holmes, R.A.W. Dryfe, Electrochemistry of Cytochrome c at the Liquid - Liquid Interface, *J. Phys. Chem. B.* 106 (2002) 12101–12103. doi:10.1021/jp026799d.